SHC 2015, International Conference on Solar Heating and Cooling for Buildings and Industry

Modeling and sizing of a MW solar DSG plant

Antoine Frein[a], Lorenzo Pistocchini[a], Victor Tatay[a], Mario Motta[a]

a Politecnico di Milano, Energy Department, Via Lambruschini 4, 20133 Milano, Itlay

Abstract

Direct Steam Generation (DSG) Concentrated Solar technology, based on Linear Fresnel Reflectors (LFR) and aimed at supplying saturated steam to industrial processes, is a promising application; nevertheless, nowadays few case studies and very few installations have been developed. A methodology for the design optimization of a MW solar DSG plant is presented in this article and applied to a real case study of a Brazilian tire manufacturing facility. A steady-state model, with spatial discretization of the ordinary equations, allows characterizing the physical phenomena such as pressure drop and heat transfer, and therefore to determine the pressure and specific enthalpy trend along the recirculation loop. For each receiver tube of the solar collectors, the occurring single or two-phase flow pattern is calculated based on specific empirical equations developed for evaporation in horizontal tubes. Two reference operating conditions have been identified for the present case study, at which the optimal field layout results to be a series connection of all the collectors, and the optimal nominal flow rate to avoid possible harmful operating conditions for the absorber tubes is 1.0 kg/s.

Keywords: Solar concentration;Process heat; Direct Steam Generation; flow pattern; Linear Fresnel Reflector; modeling and optimization

1. Introduction

The potential benefit of using solar heat above 120°C in industrial processes has already been acknowledged [1]. In fact, the European Solar Thermal technology Platform [2] highlights the huge potential of industrial process heat: 19% of the overall energy demand in the EU27 countries originates from heat used in the industrial sector. Out of such heat, 27% is in the range of 100°- 400°C. Only two commercially mature renewable technologies can reach such a range of temperatures: biomass and concentrating solar technologies, the latter providing advantages in terms of environmental impact (no dust production) and energy supply (no need for purchasing the fuel). Thus, the market potential for this technology is very large.

Steam is the most used heat transfer medium in industrial applications, thus Direct Steam Generation (DSG) heavily simplifies solar integration. Moreover, Concentrated Solar Power (CSP) applications show large

performance improvement and a reduction of the investment cost and environmental constraints, if DSG technology is used [2]. Nevertheless, this is far from being a mature technology for industrial applications: in the last five years, in the knowledge of the authors only three projects of solar DSG for industrial process have been developed:

- a 108 m^2 parabolic trough solar plant is in operation since July 2010 in an aluminum anodizing plant [3];
- 1200 m^2 of Linear Fresnel Reflectors were commissioned at the end of 2014 for a brick manufacturing [4];
- 396 m^2 of Linear Fresnel Reflectors have been commissioned in May 2015 by a pharmaceutical company in Jordan [5].

Indeed, biphasic flow requires a specific optimization to limit the pressure losses, maximize the heat transfer rates and avoid the harmful flow patterns, such as the stratified and the dry-out pattern [6]. In fact, the latter cause a thermal stress on the absorber tube , since the low heat transfer rate in the dry region can imply a dis-uniform temperature distribution (stratified flow pattern) or a very high tube temperature (dry-out region). At high temperature, the different thermal dilatation between absorber tube and glass cover could damage the sealing and compromise the vacuum. It must be also considered that even the "wavy stratified pattern" can imply (to some extent) dis-uniform temperature distributions, as some regions of the absorber are in contact only with steam.

We here present the optimization process of a MW solar DSG plant, based on a numerical model that we developed on purpose. The plant at issue is a case study: it would be integrated in the existing steam line at 20 bar-g of a tire manufacturing facility in Brazil. The solar field is made of 16 Linear Fresnel Reflectors with vacuum absorber, with an overall collector surface of 2400 m^2, and would be installed in Feira de Santana, in the region of Bahia. The technical characteristics of the solar plant, which are the starting point of the optimization process, are reported in Table 1.

The integration concept foresees an interaction at the supply level, i.e. this is the SL_S_PD integration concept, according to the classification of the IEA SHC Task 49 [7]. Practically, the saturated steam generated by the solar plant would be integrated into the process steam line, so the solar field operates in parallel to the existing steam boiler. Thus, generally speaking, the maximum solar steam generation cannot exceed the modulation capacity of the steam boiler. For the present case study we selected the "recirculation mode" operation and the related plant layout, whose outline is shown in Fig. 1, since it guarantees higher thermal-hydraulic stability and controllability, as proved by the DISS project for super-heated steam generation [8].

Nomenclature

CSP	Concentrate Solar Power	
LFR	Linear Fresnel Reflectors	
DSG	Direct Steam Generation	
IAM	Incidence Angle Modifier	
$\dot{Q}$	Heat flow rate	[kW]
$\dot{m}$	Mass flow rate	[kg/s]
P	Pressure	[Pa]
h	Specific enthalpy	[kJ/kg]
T	Fluid temperature	[°C]
θ	Wall temperature	[°C]
D	Diameter, *pipes/absorber*	[m]
dp	Linear pressure drops	[Pa/m]
α	Heat transfer rates	[kW/K.m^2]

Subscripts

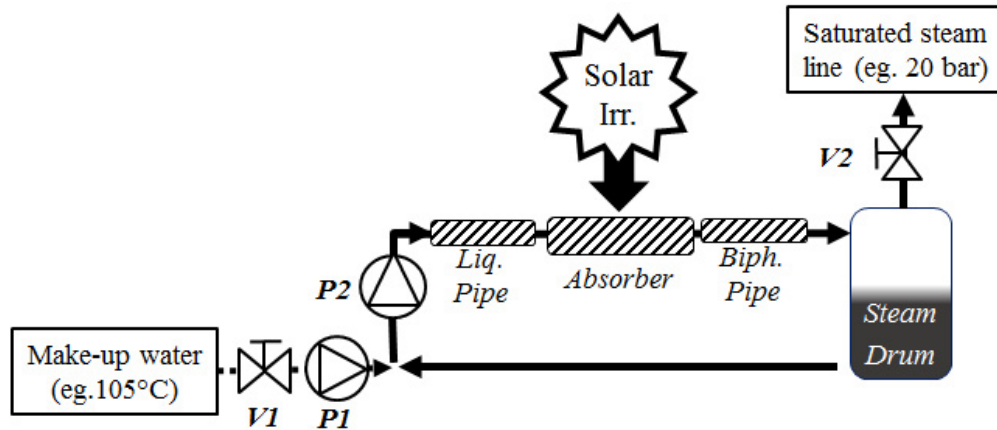|	
L	saturated liquid
V	saturated steam
i	node number

Fig. 1. Solar plant outline based on the recirculation loop concept.

Table 1. Technical features of the case study

Latitude	-12.26	[°]
Longitude	-38.95	[°]
Saturated Steam line pressure	20	[bar]
Make-up water temperature	105	[°C]
Number LFR	16	[-]
Reflector Area	2371	[m^2]
Optical efficiency	0.66	[-]
IAM coefficients	LFR manufacturer data sheet	[-]
Coefficient 1 Thermal loss evacuated tube(U_1)	0.1789 x 10^{-3}	[kW/mK]
Coefficient 2 Thermal loss evacuated tube (U_4)	7.6335 x 10^{-12}	[kW/mK^4]
Length absorber (L_{abs})	385	[m]
Diameter absorber (D_{abs})	0.066	[m]
Distance solar field – integration point	150	[m]
Diameter liquid pipe (D_L)	0.0531	[m]
Diameter biphasic pipe (D_{Bi})	0.0806	[m]
Overall linear heat transfer coefficient for liquid pipe (U_{1L})*	0.2190 x 10^{-3}	[kW/mK]
Overall linear heat transfer coefficient for biphasic pipe (U_{1Bi})*	0.2359 x 10^{-3}	[kW/mK]

*The pipe insulation thickness has been designed equals to the pipe diameter, with a conductive heat transfer coefficient of 0.04 W/mK and a convective heat transfer coefficient of 13 W/m^{2}K.

2. Research goals

Given the boundary conditions of the project, such as the nominal size of the solar field and the layout of the available space, some design and operating parameters have been analyzed to identify the optimum plant configuration. In particular, the water/steam mass flow rate and the number of parallel rows of collectors affect the pressure characteristic curve of the field, the steam quality and flow patterns.

2.1. Identification of nominal and extreme operating conditions

A methodology to select the nominal and extreme operating conditions is here proposed. In the extreme scenario, hereafter called Case 1, the highest steam quality can be achieved. This occurs during start-up operations under high irradiation. Indeed, during the start-up no feed-in water is supplied to the loop, thus the fluid at the inlet of the absorber tubes is the saturated liquid from the drum. The other scenario, called Case 2, represents nominal conditions where saturated steam is supplied to the process line, and an equivalent mass flow rate of water is fed into the recirculation loop. The operating conditions of Case 1 and 2 are reported in Table 2. The solar gain values we considered in such scenarios have been calculated on the basis of the irradiance values which occur for a defined percentage of the yearly running hours of the solar plant. A running hour occurs when the solar gain allows achieving a minimum electrical COP=20.

Table 2. Case 1 and 2: operating conditions

Model input	Case 1	Case 2
Drum Pressure	15 bar-a	22 bar-a
Solar gain	10% of the running hours	25% of the running hours
$\dot{m}_{feed-in}$ of make-up water	0 kg/s	$\dot{m}_{feed-in} = \dfrac{\dot{Q}_{tot} - \dot{Q}_{L,tot}}{h_V(P_{Drum}) - h_{feed-in}} = 0.40 \, kg\!/\!s$
$T_{feed-in}$ of make-up water	-	105 °C
T_{amb}	25 °C	25 °C

2.2. Mass flow rate analysis

Mass flow rate is a critical parameter and needs a specific optimization, particularly in a solar system where operating conditions are variable. In the present analysis we had a lower steam quality target than the value suggested by Eck et al. (0.7÷0.8), which is recommended for CSP applications since it allows the use of different type of separators (cyclone and baffle) and enables superheated collectors to be run in their ideal operation ranges [9]. Lower steam quality means a high flow rate, so the risk of harmful flow patterns - stratified and dry-out - can be avoided. On the other hand, an excessive mass flow rate results in large electricity consumptions due to the pump, and the need for a large liquid pipe diameter. At high flow rate the intermittent and wavy-stratified are the main flow patterns. The optimization process to find the suitable mass flow rate has been done under constant boundary conditions (irradiation, pressure and diameter) in the two scenarios defined above.

2.3. Solar Field layout - number of parallel rows

Once the number of LFR has been defined, the solar field layout has to be optimized: as mentioned above, the pressure drop should be minimized, harmful flow pattern avoided and the thermal performance maximized. However, the instability of transient flows of evaporating fluid in parallel pipes must be considered, since it can require more complex control systems [10].

2.4. Circuit characteristic curve

The circuit characteristic curve can be a critical issue in case of solar DSG: the Ledinegg instability [11] can occur when dealing with centrifugal pumps because of the simultaneity of variable operating conditions (due to the solar source) and evaporation. Practically, an increase of solar radiation involves the raises of both the steam quality and pressure losses, so the mass flow rate decreases accordingly. In turn, this entails a further increase of the steam quality and related pressure losses that can be greater than the reduction of pressure drop in the liquid phase, which is due to the lower mass flow rate.

As a result, the flow rate in the recirculation loop is further reduced, so the operating point of the whole plant could be highly modified by a little variation of the irradiance. Such a critical condition should be avoided.

3. Model description

Several steady-state numerical models have been developed in the framework of DSG for CSP applications, to evaluate the pressure drop and two-phase flow patterns in absorber tubes [12, 13, 14]. These models investigate the critical operating conditions and have been used to optimize steady-state operation, but they are all focused on power generation, thus on different boundary conditions: super-heated steam, large solar field, high pressure. Moreover, flow pattern correlations are always based on the formula of Tailtel and Dukler [15], which was developed in case of adiabatic two–phase flows rather than for diabatic processes of evaporation or condensation.

Therefore we implemented a new steady-state model, suitable to the operating conditions of our case study. It is based on a spatial discretization of the ordinary differential equations, and allows to analyze the physical phenomena within the absorber tube, as pressure losses and heat transfer, so to determine the trend of pressure and specific enthalpy along the recirculation loop. For each receiver tube of the solar collectors, the occurring single or two-phase flow pattern is calculated based on empirical equations developed for evaporation in horizontal tubes [16].

The main assumptions in our finite volume model are the one-dimensional approach, a homogenous distribution and thermal equilibrium of the phases within the reference volume, as shown in Fig.2.
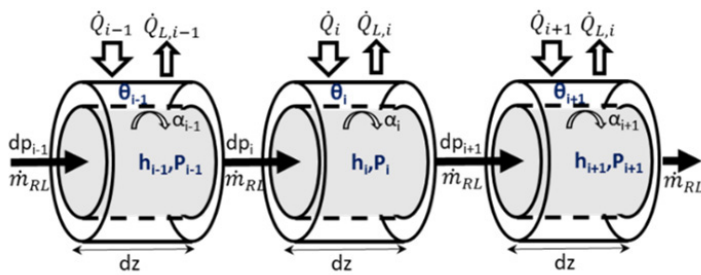

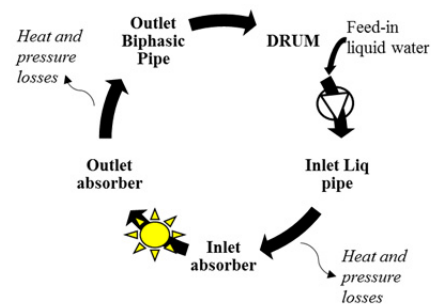Fig.2. Spatial discretization of pipes/absorber;   Fig.3. Recirculation loop

The pressure distribution along the recirculation loop is solved iteratively, by changing the hydraulic head of the pump so that the pressure at the outlet of the biphasic pipe matches the pressure in the drum, as shown in Fig. 3. In each finite volume the following system of equations is solved. Thanks to the steady state approach, the mass flow rate is considered constant throughout the loop.

$$P_i = P_{i-1} - dp_i(h_{i-1}, P_{i-1}) \cdot dz \qquad (1)$$

$$h_i = h_{i-1} + \frac{\alpha_i(h_{i-1}, P_{i-1}) \cdot [\theta_i - T_i(h_i, P_i)] \cdot dz \cdot \pi \cdot D}{\dot{m}_{RL}} \qquad (2)$$

$$\dot{Q}_i - \dot{Q}_{L,i}(\theta_i) = \alpha_i(h_{i-1}, P_{i-1}) \cdot [\theta_i - T_i(h_i, P_i)] \cdot dz \cdot \pi \cdot D \qquad (3)$$

$$\dot{Q}_{L,i}(\theta_i) = U_1 \cdot \theta_i + U_4 \cdot \theta_i^4 \qquad (4)$$

The coefficients dp_i (linear pressure drop) and α_i (heat transfer rate) are calculated for each finite volume i, on the base of the fluid dynamics in the previous volume i-1. The linear pressure drop is calculated by the Petukhov correlation [17] for liquid phase, whereas the Friedel correlation [17] is applied in case of biphasic flows. Concerning the heat transfer rate, in the single (liquid) phase it is calculated by the Gnielinski correlation [18], being the Reynolds number in the range $[2.3 \cdot 10^3; 5 \cdot 10^6]$. In the biphasic flow, the Kandlikar correlation [18] is applied up to the dry-out region (high steam quality), then the Bowring formula [18] is used.

For the liquid and biphasic pipes, that is the pipings respectively upstream and downstream the solar field, the same equations are used with some small adjustment: solar heat gain is zero, U_1 is calculated on the base of insulation thickness, U_4 is neglected. Moreover, a less dense discretization is applied, consisting in just one node for the liquid pipe and five nodes for the biphasic pipe.

Once pressure, temperature and steam quality distribution have been calculated for the whole recirculation loop, the flow pattern in each collector is analyzed. Historically, flow pattern maps were built for adiabatic two-phase flows [15]. In more recent years, new flow patterns specific to evaporation in horizontal tubes have been developed by Kattan, Thome and Favrat (KTF) [16], and tuned for refrigerant in small-diameter pipes. In the present study, the KTF maps have been adapted to water flow in larger diameter pipes (DN 65 vs DN 20).

4. Results

4.1. Definition of the boundary conditions

The graph in Fig. 4 is an irradiance duration curve, related to the site of the solar plant. In the graph, the resulting solar gain duration curve (the dashed one) is reported. This is determined by the numerical model, and depends on the solar field performances. By simulating the plant during start-up operation, with a drum pressure of 15 bar, no feed-in water integration and a mass flow rate of 1.0 kg/s, we calculated the minimum useful solar gain, which guarantees an electrical COP = 20. This is an optical gain of 30 W/m^2, which implies a net overall solar gain of 30 kW_{th}, against a pump consumption of about 1.5 kW_e. At such a minimum value of the solar gain we assume that the plant is switched on. In the graph in Fig. 4 we report also the solar gain values related to Case 1 and Case 2, and mentioned in Table 2.
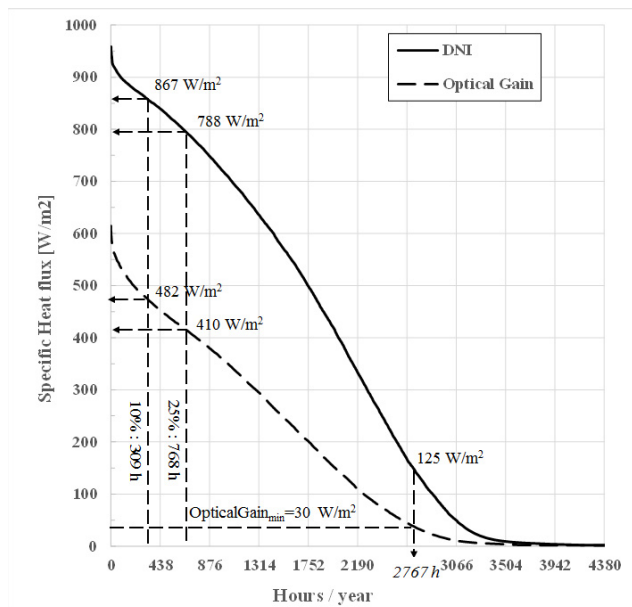

Fig. 4. Irradiance duration curve, based on monitored data of year 2012 at Petrolinas [19].

4.2. Optimal mass flow rate

Based on the analysis of flow pattern, an optimal range for the mass flow rate rather than an optimal value has been defined. In Case 1, shown in Fig. 5, this range is between 1 kg/s and 2 kg/s: the superheated steam is avoided and stratified flow pattern is minimized. Furthermore, to maximize the annular region, the stratified wavy region should be increased. In Case 2 in Fig. 6, the same range can be used, as large stratified wavy flow pattern occurs at a lower mass flow rate.
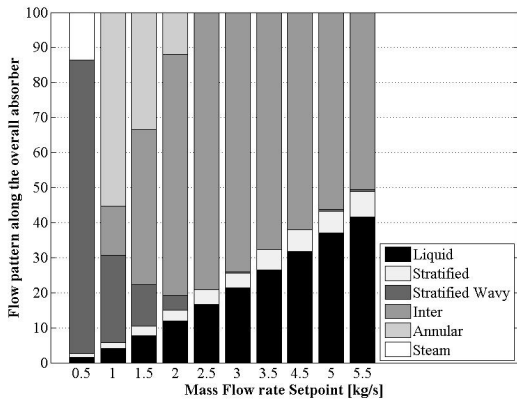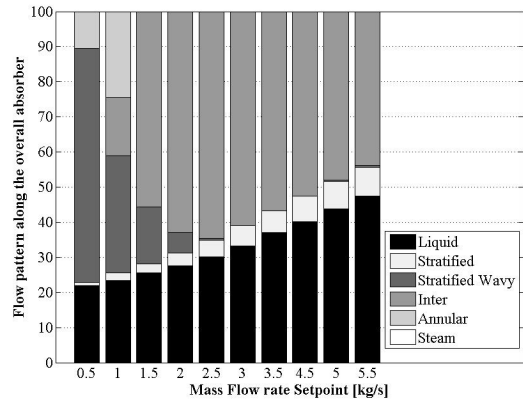
Fig. 5. Flow pattern distribution in Case 1;

Fig.6. Flow pattern distribution in Case 2;

The KTF map can effectively show the flow pattern according to the specific mass flow rate and the steam quality. An example, related to Case 1, is presented here below in Fig. 7.
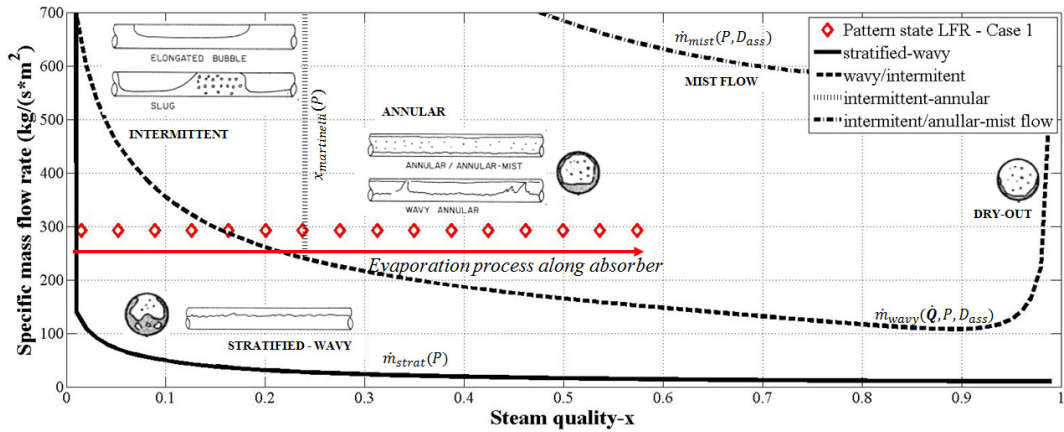

Fig.7. Average fluid conditions for each LFR (red diamond) for Case 1 and a flow rate of 1 kg/s on KTF flow pattern map [16]

4.3. Solar Field layout

The results presented in Fig. 5 and 6 are related to a specific solar field layout, where all the LFR are in series. A two-row configuration has been investigated too (the outline is reported in Figure 8), and the results are shown in Fig. 9 and 10. We assumed that the overall mass flow rate is equally distributed.
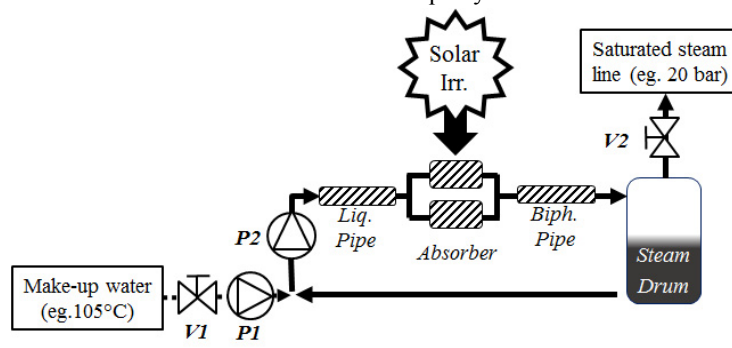

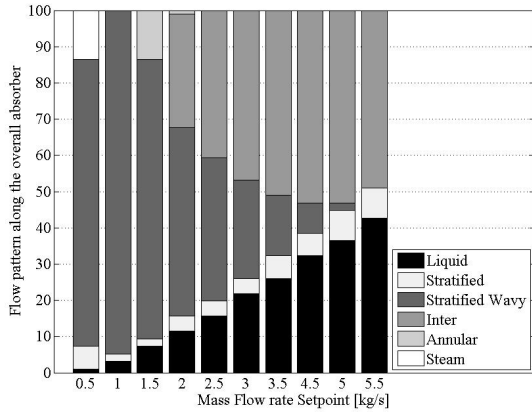Fig. 8. Parallel configuration of solar field

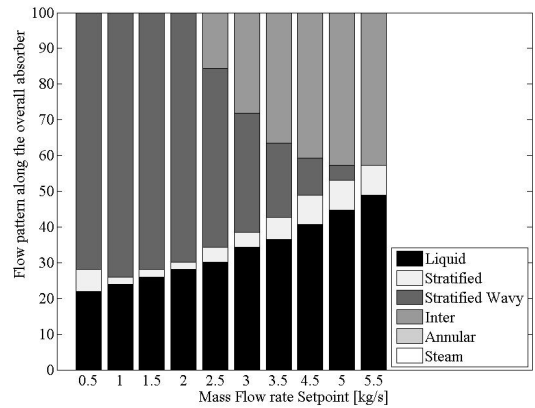Fig. 9. Flow pattern distribution in Case 1;

Fig.10. Flow pattern distribution in Case 2;

In the present case study, the parallel layout is not suitable as the mass flow rate should be drastically increased to avoid a large share of stratified wavy pattern, moreover the annular flow pattern cannot be obtained. Thus, to maintain a satisfactory flow pattern distribution the pressure drop of the overall system is increased: losses in the absorber tubes have the same order of magnitude, but those in the liquid and biphasic pipes strongly increase.

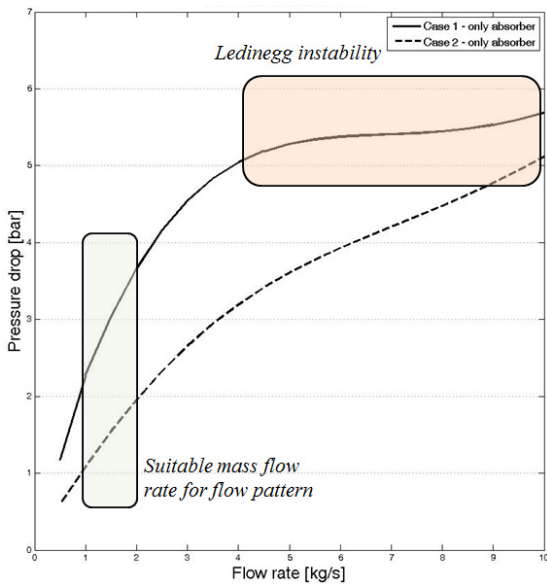### 4.4. Characteristic curve

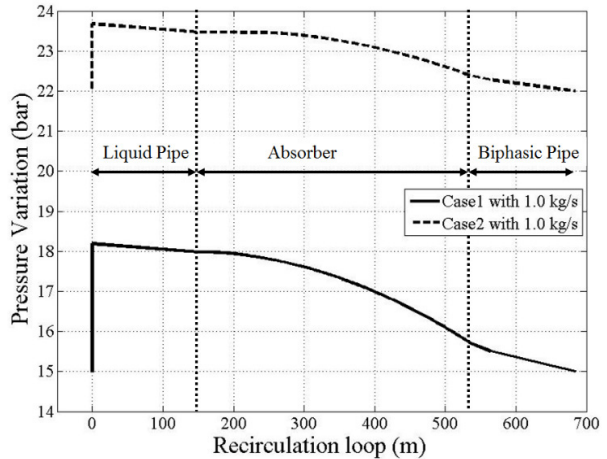Fig. 11. Characteristic curve for Cases 1 and 2;

Fig.12. Pressure distribution along the recirculation loop, at 1.0 kg/s

The circuit characteristic curve related to Case 1 shows Ledinegg instability for a flow rate between 4 and 10 kg/s, as indicated by the graph in Fig. 11. Nevertheless, such instability does not affect the pump control, since in the optimal range of flow rate resulting from the flow pattern analysis (i.e. 1.0 to 2.0 kg/s) the curve slope is steep. The instability does not occur at all in Case 2, since the liquid region represents a large share of the overall absorber tubes length (at least 20%, as shown in Fig. 6), so a flow rate reduction, which involves a pressure drop reduction in the liquid phase proportional to the square root of the flow rate, affects the overall pressure drop more than the higher losses due to the increased steam quality. To minimize the pressure drop, a flow rate of 1.0 kg/s has been chosen for Case 2. The pressure distribution along the whole recirculation loop is presented in fig.12 for both Case 1 and 2.

5. Further results of optimization work

5.1. Simplification of numerical model

In the numerical model here presented, the heat transfer rate is calculated for each node and based on specific correlations according to the fluid condition, as shown in Fig. 13 for Case 2. Given the solar radiation, the heat transfer rate determines the temperature difference between the wall and the fluid. A higher wall temperature means higher thermal losses. Anyway, thanks to the effective insulation of absorber tubes, the impact of the increase of wall temperature on overall losses is limited. So, by using the correlation for liquid flow in the whole recirculation loop – as done in the simulation reported by Fig. 14 – the computational effort is much reduced, and the overall net solar gain is underestimated just by 0.05% in Case 2.
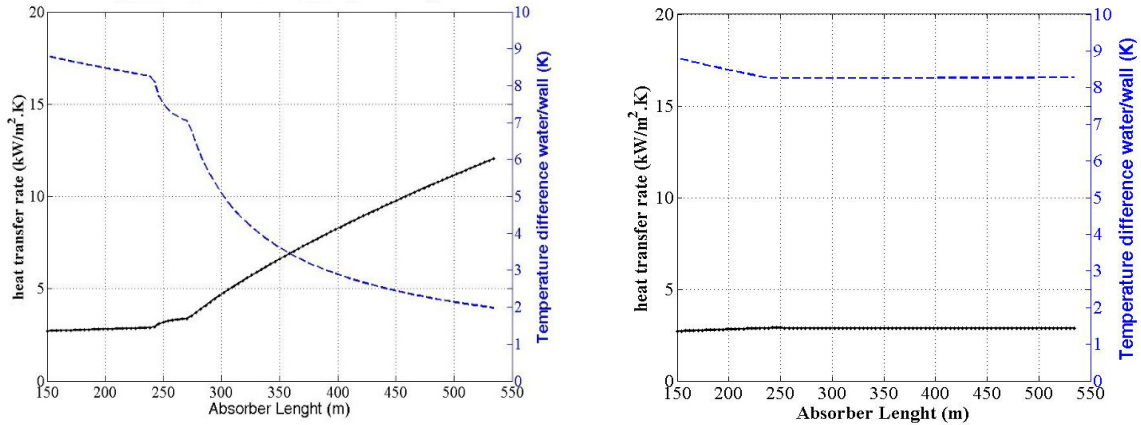

Fig. 13. Variable Heat transfer rate and resulting temperature difference; Fig.14. Constant Heat transfer rate and resulting temperature difference;

5.2. Variable absorber tube diameter to minimize the harmful flow pattern

As shown in Fig. 5 and 6, the tube length where wavy stratified flow pattern occurs cannot be reduced by varying the flow rate without decreasing also the length of annular flow pattern. A way to overcome this problem can be the use of different absorber tube diameters, in order to increase the specific mass flow rate just in the first section of the solar field. For example, with a mass flow rate of 1.0 kg/s, if the diameter of the first 200 m of absorber tubes is reduced by 20%, from 53 mm to 66 mm, the tube length affected by wavy stratified pattern is reduced by 81% in Case 1, and by 61% in Case 2, as shown in Fig. 15.
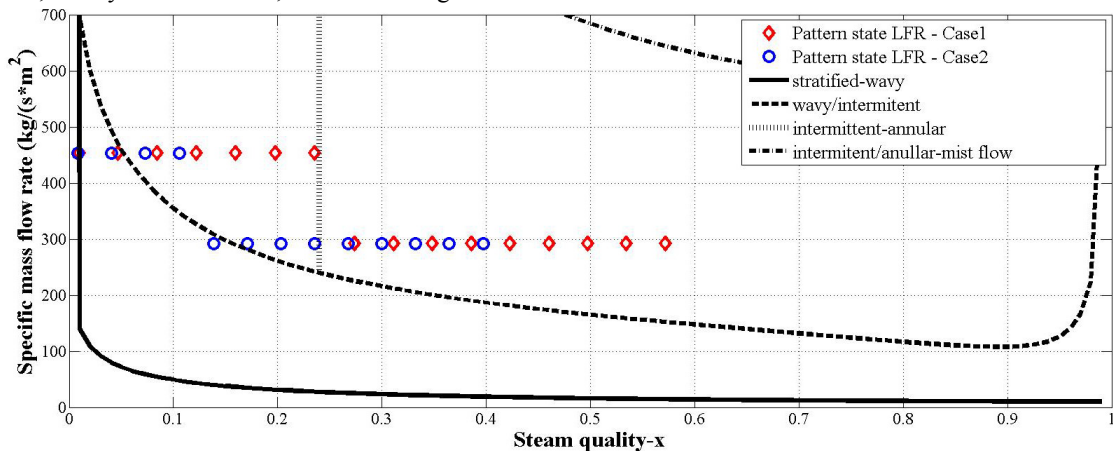

Fig15. Average fluid conditions for each LFR with variable absorber diameter, at 1 kg/s flow rate, on KTF flow pattern map [16].

6. Conclusions

We have presented an optimization process of a MW solar DSG plant, which would be integrated in a real tire manufacturing facility in Brazil. The design optimization is based on the analysis of flow patterns and pressure drop, in two selected operating conditions. The analysis tool is a numerical model, developed on purpose. Different field layouts have been investigated: the solar plant where all the solar collectors are connected in series results to be a better choice than any configurations with parallel connections, mainly due to control issues.

The flow pattern analysis has shown that for the present case it is not possible to avoid completely the harmful flow patterns while maximizing the annular flow pattern. Nevertheless, by a mass flow rate of 1.0 kg/s the best flow patterns for system operation occur in a large share of the absorber tubes, and the Ledinegg instability is avoided. This result can be even improved by using two different absorber diameters for the regions with low and high quality of the steam.

Further work should be done to experimentally validate the adaptation of the KTF correlations to the present case. Moreover, a study of the dynamics of the plant operation during start-up turns out to be necessary to the correct sizing of the steam drum, which is a main component of the plant.

Acknowledgements

References

[1] Solar Heating & Cooling programme of the International Energy Agency, *Solar Heat Worldwide – Markets and contribution to the energy supply 2012*, 2014.

[2] Feldhoff, J. F., Schmitz, K., Eck, M., et al., *Comparative system analysis of direct steam generation and synthetic oil parabolic trough power plants with integrated thermal storage*, Solar Energy, 86 (1),2012, pp. 520-530

[3] D. Krüger,N. Lichtenthäler,J. Dersch,et al, *Solar steam supply: initial operation of a plant*, ISES Solar World Congress, Sept 2011.

[4] Vittoriosi A., Fedrizzi R., Brock R., Orioli F., Orioli V., Pietruschka D., *Monitoring of a MW Class Solar Field Set Up in a Brick Manufacturing Process*, Energy Procedia 48, 2014, 1217–1225

[5] Martin Haagen, et al, *Solar process steam for pharmaceutical industry in Jordan*, SHC 2014, Energy Procedia 70, 2015, 621 – 625

[6] Thome J.R., *Engineering Data Book III chapter 12: Two-Phase Flow Patterns*, Wolverine Tune, Inc., 2004-2006

[7] Muster Bettina,et al, *Integration guideline,* Solar process heat for production and advanced application, delivreable B2 - IEA SHC Task 49

[8] Eck M, Zarza E, Eickhoff M, Rheinlander J, Valenzuela L. *Applied research concerning the direct steam generation in parabolic troughs,* Solar Energy 2003;74:341–51.

[9] Eck M, Schmidt H, Eickhoff M, Hirsch T., *Field test of water-steam separators for direct steam generation in parabolic troughs.* SolarPACES2006 A1-S5

[10] Taitel Y., Barnea D., *Transient solution for flow of evaporating fluid in parallel pipes using analysis based on flow patterns*, International Journal of Multiphase Flow 37 (2011) 469–474

[11] Dagan, E., Muller M., and Lippke F., 1992, 'Direct Steam Generation in the Parabolic Trough Collector, Report of Plataform Solar de Almeria-Madrid.

[12]Jie Sun, Qibin Liu, Hui Hong, *Numerical study of parabolic-trough direct steam generation loop in recirculation mode: Characteristics, performance and general operation strategy*, Energy Conversion and Management 96 (2015) 287–302

[13] Odeh SD, Behnia M, Morrison GL. *Hydrodynamic analysis of direct steam generation solar collectors.* Solar Energy Engineering, ASME 2000;122:14–22.

[14] Odeh SD, Behina M, Morrison GL. *Hydrodynamic model for horizontal and inclined solar absorber tubes for direct steam generation collectors.* In: 13th Australian Fluid Mechanics Conference, Melbourne, Australia. 1998. p. 969–72.

[15] Taitel, Y., and Dukler, A. E., 1976, *A model for predicting flow regime transitions in Horizontal and near horizontal gas-liquid flow*, AIChE Journal, 22 (1), pp. 47-55.

[16] Kattan N., Thome J.R and Favrat D. *Flow boiling in horizontal tubes, Part 1, development of a diabatic two-Phase flow pattern Map*, J. Heat transfer, Vol 120, N0. 1, 1998a, pp140-147.

[17] F. Incropera and D. DeWitt, *Fundamentals of Heat and Mass Transfer*. Wiley, USA, 4 edition, 1996.

[18] Collier J.G., Thome J.R, *Convective Boiling and condensation*, third edition, Clarendon press Oxford, 1996.

[19] INPE, SONDA, Sistema De Organizacao Nacional de Dados Ambientais, http://sonda.ccst.inpe.br/basedados/petrolina.html, 2012.